Journal of Nanoparticle Research (2005) 7: 555–567
DOI 10.1007/s11051-005-5674-z

Uptake and sequestration of naphthalene and 1,2-dichlorobenzene by C_{60}

Xuekun Cheng, Amy T. Kan* and Mason B. Tomson
*Department of Civil and Environmental Engineering, Rice University, MS-519, 6100 Main Street, Houston, TX 77005, USA; *Author for correspondence (Tel.: +1-(713) 348-5224; Fax: +1-(713) 348-5203; E-mail: atk@rice.edu)*

Received 14 April 2005; accepted in revised form 18 April 2005

Key words: carbon nanomaterials, C_{60}, nano-C_{60}, environmental impact, PAH, desorption hysteresis, colloids, water quality

Abstract

The interactions of common environmental contaminants with C_{60} have been studied to evaluate the environmental impact of carbon nanomaterials. The adsorption and desorption interaction of the hydrophobic contaminants naphthalene and 1,2-dichlorobenzene with C_{60} was characterized. Processes that cause the wetting and disaggregating of C_{60} particles also affect the extent of organic contaminant sorption to C_{60} aggregates by orders of magnitude. C_{60} dissolved in organic solvents such as toluene can form stable nanoscale aggregates upon vigorous mixing in water. These nanoscale C_{60} particles form stable suspensions in water and are referred to as 'nano-C_{60}'. Desorption of contaminants from stable suspensions of nano-C_{60} exhibits hysteresis. The experimentally observed adsorption/desorption hysteresis is described by a two-compartment desorption model: first, adsorption to the external surfaces that are in contact with water, and second, adsorption to the internal surfaces within the aggregates.

Introduction

Carbonaceous nanomaterials, such as single wall nanotubes and fullerenes, have attracted a great deal of attention due to their unique physical/chemical and mechanical properties. Researchers continue to find new applications of these materials in energy, medicine, space, information technology, industrial and environmental applications, to mention a few. While large scale production of these materials has begun, environmental scientists as well as the public have concerns about their environmental impacts (Borm, 2002; Dagani, 2003). Therefore, it is necessary to investigate the fate and transport of these materials to determine possible adverse environmental impacts and to help establish guidelines for application and disposal of these materials.

Many soils or sediments contain various forms of carbonaceous materials such as biogenic materials, humic substances, coals, kerogens, and black carbons (e.g., soot and char) (Allen-King et al., 2002). Black carbons form mostly through incomplete combustion of either plants or fossil fuels (Setton et al., 2002). All of these carbon materials contain stacks of 6-carbon aromatic rings. C_{60} was originally discovered while producing soot (Kratschmer et al., 1990). Instead of having 6-carbon ring arranged in sheet, C_{60} contains both 6- and 5-carbon rings, arranged in a spherical configuration. Kerogens, coals, and black carbons have been reported to have much higher affinity for hydrophobic organic contaminants than humic substances (McGroddy & Farrington, 1995; Chiou & Kile, 1998; Bucheli & Gustafsson, 2000; Accardi-Dey & Gschwend,

2002; Kleineidam et al., 2002; Braida et al., 2003; Chun et al., 2004; Nguyen et al., 2004; Zhu et al., 2004; Cornelissen & Gustafsson, 2005; James et al., 2005). The existence of a small fraction of coal, kerogen, and/or black carbon in nature has been of great concern for transport and bioavailability of organic contaminants (Goldberg, 1985; McGroddy et al., 1996; Gustafsson et al., 1997; Bucheli & Gustafsson, 2000; Ghosh et al., 2003).

The focus of this research is to investigate the adsorptive/desorptive properties of environmental pollutants to aqueous dispersions of C_{60}. C_{60} is practically insoluble in water (Ruoff et al., 1993). The formation of aqueous aggregates of C_{60} in polar media has been reported in many studies (Andersson et al., 1992; Scrivens et al., 1994; Andrievsky et al., 1995; Mchedlov-Petrossyan et al., 1997; Brettreich & Hirsch, 1998; Jenekhe & Chen, 1998; Lai et al., 2000; Sano et al., 2000). C_{60} can be dispersed in water after stirring for 2 days (Cheng et al., 2004). In some cases, additives, e.g., surfactants, cyclodextrins, or sugar polymers, have been used to disperse C_{60} in water (Andersson et al., 1992; Beeby et al., 1994; Bensasson et al., 1994). C_{60} can also be dispersed in water by first dissolving it in an organic solvent, then adding the solution to water and evaporating-off the organic solvent (Scrivens et al., 1994; Andrievsky et al., 1995; Wei et al., 1997; Alargova et al., 2001; Deguchi et al., 2001). Sorption and desorption are important processes that control the fate and transport of both nanoparticles and environmental contaminants. Since nanomaterials provide large surface areas, they may be strong sorbents for many contaminants. The fate of hydrophobic organic pollutants are controlled largely by the carbonaceous matter in soil (Chiou et al., 1979; Karickhoff et al., 1979; Steinberg et al., 1987; Pignatello, 1989; Pignatello & Xing, 1996; Kan et al., 1998; Weber et al., 1998; Accardi-Dey & Gschwend, 2002; Kleineidam et al., 2002; Cornelissen & Gustafsson, 2005). Hysteretic desorption of organic compounds from soil and sediments has been observed in many studies (Di Toro & Horzempa, 1982; Pignatello & Huang, 1991; Kan et al., 1994; Huang & Weber, 1997; Huang et al., 1998; Kan et al., 1998; Weber et al., 1998; Xia & Pignatello, 2001; Braida et al., 2003). Hysteresis has also been observed for desorption of organic vapor molecules from C_{60} lattice (Rathousky et al., 1993; Rathousky & Zukal, 2000). One objective of this paper is to test if hysteresis occurs when organic contaminants desorb from C_{60} particles in aqueous solutions.

Although a large number of reports have addressed the physical/chemical and mechanical properties of C_{60}, only a few studies have discussed the adsorption of organic compounds from aqueous solution to C_{60} solids (Ballesteros et al., 2000; Mchedlov-Petrossyan et al., 2001). The present authors have shown that when black C_{60} powder is dispersed in water and gently tumbled, the particles formed are from 20 to 50 μm in diameter (called, 'C_{60} large aggregates'), but when the powder is stirred vigorously with a magnetic stirring bar for 2–3 days, the particles formed are 1–3 μ m in diameter (called, 'C_{60} small aggregates') (Cheng et al., 2004). In this study, adsorption and desorption of naphthalene and 1,2-dichlorobenzene to nanometer-sized C_{60} aggregates (nano-C_{60}) have been studied and compared to that of larger C_{60} particles and black carbon. Nano-C_{60} particles are underivatized C_{60} crystalline nanoparticles containing 100–1000 C_{60} molecules (Colvin, 2003; Lecoanet & Wiesner, 2004; Sayes et al., 2004). These nano-C_{60} particles acquire a negative charge, which contributes to their suspension stability in water (Mchedlov-Petrossyan et al., 1997; Deguchi et al., 2001; Mchedlov-Petrossyan et al., 2001). Aqueous suspensions of nano-C_{60} in 0.05 M ionic strength or below, are stable for months (Scrivens et al., 1994; Mchedlov-Petrossyan et al., 1997; Andrievsky et al., 1999; Deguchi et al., 2001). The size distribution of these aggregates is affected by the formation condition, e.g., mixing speed (Fortner et al., 2005).

Materials and methods

Materials

C_{60} solids (purity >99.5%) were purchased from SES Research (Houston, TX, USA). ^{14}C-radiolabeled naphthalene and ^{14}C-radiolabeled 1,2-dichlorobenzene (1,2-DCB) with specific activities of 8.1 μCi/μmol and 8.8 μCi/μmol, respectively, were purchased from Sigma-Aldrich (St. Louis, MO) and were diluted in methanol (HPLC grade) to make stock solutions. Toluene was purchased from Sigma-Aldrich with a purity of 99.8%.

Tetrahydrofuran (THF, HPLC grade) used in this study was kept in the dark and was purged with nitrogen after each use to prevent oxidation. Ready Safe or Ready Organic liquid scintillation cocktails for scintillation counting were supplied by Beckman Instruments, Inc. (Fullerton, CA). Anodisc® filter membranes (20 nm pore size, Whatman) were used to separate nanoscaled C_{60} particles from solution. The filter membrane is made of a high purity alumina matrix that is manufactured electrochemically. It has a precise, non-deformable honeycomb pore structure with no lateral crossovers between individual pores and therefore a sharp molecular weight cut-off.

Preparation of nano-C_{60} in water

Stable aqueous suspensions of nano-C_{60} particles were prepared by two different methods, similar to those described by Andrievsky et al. (1995) and Deguchi et al. (2001) and referred to as 'sonication' and 'THF' methods, respectively. For the sonication method, a solution of 560 mg/l C_{60} was first prepared in toluene at room temperature. The solubility of C_{60} in toluene is 2800 mg/l (Taylor, 1999). A total of 100 ml of 560 mg-C_{60}/l toluene solution was added to the top of 200 ml of deionized water in a beaker. The mixture was then subjected to continuous sonication with a high-energy sonication probe (Sonifier® Cell Disruptor, W185D, Heat Systems-Ultrosonics, Inc., Farmingdale, NY) for about 4 h in the dark until the mixture changed from a purplish emulsion to a yellowish suspension and the purple toluene layer on the top of the suspension evaporated. During the course of ultrasonic evaporation, a large fraction of C_{60} aggregates (46.4 mg) was deposited to the inner wall or the bottom of the beaker instead of being incorporated into nanoscale aggregates in water. The resultant nano-C_{60} suspension was cooled and was filtered through glass fiber (1 μm nominal pore size, Fisherbrand, Fisher Scientific.) to remove larger aggregates. The filtrate contained 48 mg/l of stable nano-C_{60} suspension in water.

For the THF method, about 100 mg of C_{60} was added into 4 l THF. The solution was sparged with nitrogen (Matheson UHP grade, 99.999%) for 30 min and then sealed tightly and stirred overnight in the dark to dissolve C_{60}. The C_{60} solubility in THF is approximately 9 mg/l (Deguchi et al., 2001). A 500 ml sample of the C_{60}/THF solution was then filtered with a 0.22 μm nylon filter membrane (GE Osmonics Inc.) to remove undissolved C_{60} and sparged with nitrogen for 15 min. Deionized water, 500 ml, was then added at a flow rate of about 1000 ml/min to the C_{60} saturated THF solution with vigorous mixing. The suspension was transferred into a rotary evaporator (Buchi Rotavapor R-200, Buchi Labortechnik AG, Flawil, Switzerland) to evaporate the THF. When the C_{60}/THF/water mixture volume was reduced to about 500 ml in about 1 h, 200 ml DI water was added into the Rotavapor and the suspension volume was again reduced to about 500 ml. The suspension was diluted with another 200 ml DI water and then the evaporation was resumed for about 30 min until the final suspension volume was reduced to about 500 ml. The final suspension was filtered through glass fiber filter membrane (1 μm nominal pore size, Fisherbrand, Fisher Scientific.) and a nano-C_{60} suspension containing 12.5 mg/l C_{60} was obtained. Another batch of the nano-C_{60} suspension was prepared by the same procedure, except that when water was added to the C_{60}/THF solution, a flow rate of about 100 ml/min was used and the suspension volume was reduced to about 100 ml by evaporation. This nano-C_{60} suspension contained 65 mg/l of C_{60}.

The particle sizes of nano-C_{60} were measured by photon correlation spectroscopy (PCS System 4700 C, Malvern Instruments Inc., Southborough, MA). Concentrations of nano-C_{60} were determined by UV–Vis spectrophotometry (DR/4000, HACH Company, Loveland, CO). A standard curve was established with C_{60}/toluene solutions from 1.7 to 34 mg/l. To measure nano-C_{60} concentration, a nano-C_{60} sample was filtered with 20 nm Anodisc® filter membrane. The nano-C_{60} on the membrane was dissolved in toluene and the nano-C_{60} concentration in toluene was measured spectrophotometrically. Wavelength scan of the obtained C_{60}/toluene solution at 200–800 nm was conducted for the nano-C_{60} suspension prepared by the sonication method (C_{60} 48 mg/l). After going through naphthalene adsorption, filtration, resuspension, and desorption, the nano-C_{60} suspension was filtered and dissolved in toluene using the same procedure as described above. The obtained C_{60}/toluene solution was scanned again to compare with the spectrum of the freshly prepared nano-C_{60}.

Naphthalene adsorption and desorption with nano-C_{60}

Naphthalene adsorption and desorption experiments were conducted with nano-C_{60}. Batch reactors, consisting of EPA-certified glass vials (Fisher Scientific) with Teflon-septum caps, were used for adsorption and desorption experiments. At the beginning of the adsorption experiments, nano-C_{60} suspensions (prepared by the sonication method, C_{60} = 48 mg/l) were pipetted into seven 8-ml glass vials with PTFE septum and screw caps. A Teflon-coated micro-stir bar was placed in each vial. Different volumes of ^{14}C-radiolabeled naphthalene/methanol stock solutions were injected into the vials with a microsyringe so that the initial naphthalene concentrations were 1.10, 1.97, 2.20, 2.51, 3.30, 4.26, 5.11 μg/mL (sample numbers 1.1 to 1.7). Sample vials were closed tightly with headspace of less than 0.1 ml. The volume fraction of methanol in solution phase in each vial was less than 0.002, which is not expected to affect the naphthalene adsorption. Another seven control vials were set up the same way as the sample vials except that no nano-C_{60} was added. Control vials were designed to account for the loss of naphthalene from the aqueous phase due to volatilization or adsorption to the vessels. Sample vials and control vials were stirred slowly on magnetic stirrers in the dark at room temperature (25 ± 1°C) for 3 days. At the end of each experiment, 5 ml of sample was filtered using an Anodisc® filter membrane. 1 ml filtrate was added to Ready-Safe® liquid scintillation cocktails and analyzed for naphthalene with Beckman liquid-scintillation counter (Beckman Instruments Inc., Fullerton, CA). The retention of naphthalene by Anodisc® filter membrane was measured by filtering 5 ml of naphthalene stock solution through the membrane, measuring the naphthalene concentration of the filtrate, and comparing the filtrate concentration with that of the stock solution. Approximately 8.0 ± 0.4% of naphthalene was lost during the filtration step. Thus, for those samples in which Anodisc® filter membranes were used, experimentally measured aqueous naphthalene concentrations were divided by 0.92 to calculate the actual aqueous phase concentrations. About 1 ml of the solution in each control vial was also analyzed for aqueous phase naphthalene concentrations by liquid-scintillation counter. Naphthalene concentration in the control samples was 97.39 ± 0.11% of the original concentrations. Solid-phase naphthalene concentration in each sample vial was calculated from the difference between the solution phase naphthalene concentration in the sample vial and that in the corresponding control vial. Desorption of naphthalene from nano-C_{60} was measured for three of the seven adsorption samples (sample numbers 1.1, 1.3, 1.5). The suspension in each of these three sample vials was filtered through Anodisc® filter membrane. The membrane containing C_{60} solids was put into a clean sample vial and naphthalene-free deionized water was added to each vial. The vials were sealed and put into a sonication bath (Solid State/Ultrasonic FS-14, Fisher Scientific) for 15 min to redisperse nano-C_{60}. Membranes were then removed carefully from the sample vials. Next, deionized water was added to each sample vial (with headspace <0.1 ml) and samples were stirred in the dark at room temperature for 3–7 days. Each of the membranes was then soaked in 1 ml of toluene to dissolve retaining C_{60}. This solution was analyzed using a UV/Vis spectrophotometer to quantify the amount of C_{60} remaining on the membrane. The loss of C_{60} during each filtration step was used to correct the mass of adsorbent in the next desorption experiment. The particle size distributions of the nano-C_{60} samples were measured by photon correlation spectroscopy to determine if the particle size distribution had changed. After being stirred for 3–7 days, the suspension in each sample vial was filtered with Anodisc® filter membrane and aqueous phase naphthalene concentration was determined using liquid-scintillation counter. Three desorption steps were conducted for each of the three adsorption samples. Upon completion of the third desorption step, solid-phase naphthalene concentrations were analyzed following filtration by dissolving C_{60} solids collected on each filter membrane in toluene. A portion of the resultant C_{60}/toluene solution was analyzed by liquid-scintillation counter to obtain solid-phase naphthalene concentration. Another portion of the C_{60}/toluene solution was analyzed by UV–Vis spectrophotometry to determine C_{60} mass balance.

1,2-dichlorobenzene (1,2-DCB) adsorption and desorption with nano-C_{60}

Similar adsorption and desorption experiments of 1,2-DCB with nano-C_{60} were conducted. The

nano-C_{60} suspensions (prepared by the THF method with C_{60} concentration of 62.5 mg/l) were added to three 16-ml sample vials (sample nos. 2.1, 2.2, 2.3). A small aliquot of ^{14}C-radiolabeled 1,2-DCB/methanol stock solution was injected into each vial with a microsyringe so that the initial 1,2-DCB concentrations were 0.89, 4.65, and 8.23 μg/ml, respectively. Adsorption and three steps of desorption were conducted with each of the three samples using a procedure similar to the naphthalene adsorption/desorption experiments.

Kinetics of naphthalene desorption from nano-C_{60}

Two 16-ml sample vials (sample nos. 3.1 and 3.2) were filled with nano-C_{60} suspensions prepared by the THF method with C_{60} concentration of 12.5 mg/l. A small aliquot of ^{14}C-radiolabeled naphthalene/methanol stock solution was added into each vial so that the initial naphthalene concentrations were 8.62 and 8.67 μg/ml, respectively. Adsorption experiments were conducted using the same procedures as those for sample numbers 1.1 to 1.7. A total of three desorption steps were conducted with each of the two samples. During each desorption step, the time-dependent naphthalene desorption was monitored periodically by measuring the aqueous phase naphthalene concentrations. At each time of sampling, 100 μl of the aqueous sample was filtered and the aqueous naphthalene concentration was measured by scintillation counting. Naphthalene binding to Anodisc® filter membrane was also determined by filtering 100 μl of naphthalene stock solution through the membrane and comparing naphthalene concentration in the filtrate to that of the naphthalene stock solution. Control test results showed that naphthalene concentrations after filtration were 70.5 ± 0.62% of that in the orginal control samples. Therefore, in the adsorption/desorption experiments concentrations of naphthalene in the filtrates were divided by 0.705 to correct for the filtration losses.

Results and discussion

Nano-C_{60} in water

Suspensions of nano-C_{60} particles as prepared in this study are transparent with a yellowish color. The wavelength scan spectrum of the C_{60}/toluene solution obtained from nano-C_{60} suspension (freshly prepared from sonication method, C_{60} 48 mg/l) by UV–Vis spectrophotometer is shown in Figure 1a. The spectrum for the C_{60} after going through adsorption, filtration, resuspension and desorption processes is shown in Figure 1b. The absorption spectra showed clear C_{60} characteristic peaks at 336 nm and 407 nm wavelength, and no peak at 424 nm wavelength, which indicates the absence (to within about 1%) of C_{60} oxide (Heymann et al., 2000; Weisman et al., 2001).

Nano-C_{60} in DI water cannot be extracted from its aqueous suspension with either toluene or benzene. When nano-C_{60} was dispersed in toluene solution, an opaque emulsion formed and the toluene and water phases did not separate for 1 week. However, addition of an electrolyte, e.g., 2 wt% NaCl, will precipitate C_{60} from its aqueous dispersion (Mchedlov-Petrossyan et al., 1997; Wei

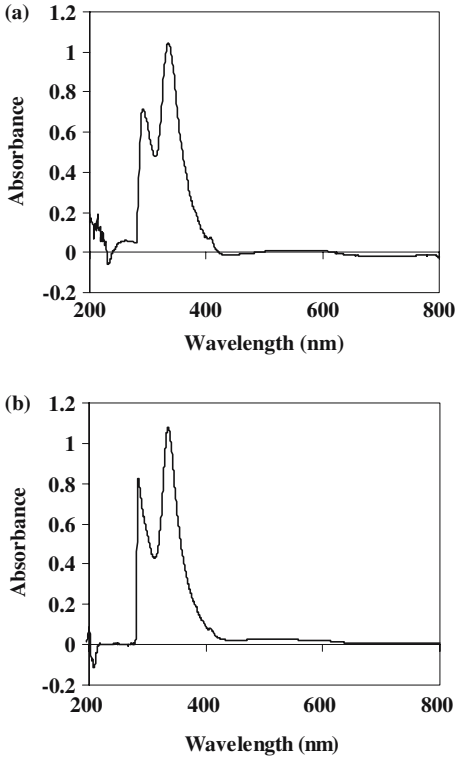

Figure 1. UV–Vis absorption spectra of C_{60} in toluene. (a) obtained from freshly prepared nano-C_{60} suspension (sonication method, C_{60} 48 mg/l); (b) obtained from nano-C_{60} suspension after going through adsorption, filtration, resuspension, and desorption.

et al., 1997; Alargova et al., 2001; Deguchi et al., 2001; Andrievsky et al., 2002). Similar results have been observed by several other researchers (Scrivens et al., 1994; Wei et al., 1997; Deguchi et al., 2001). The amount of toluene left in nano-C_{60} was measured by dissolving a sample of nano-C_{60} (by the sonication method) in methylene chloride and analyzing toluene concentration on GC/MS. Approximately 5 mg toluene/g–C_{60} was observed in nano-C_{60}. This small amount of toluene in C_{60} is not expected to affect naphthalene adsorption/desorption substantially.

Particle size distributions were determined using photon correlation spectroscopy and results are shown in Figure 2. The particle size distributions of the 48 mg/l nano-C_{60} prepared by the sonication method and 65 mg/l nano-C_{60} prepared by the THF method could be fitted with a normal distribution equation. The mean particle diameter of nano-C_{60} produced by the sonication method (48 mg/l) was 170.3 ± 30.2 nm ($R = 0.993$) (Figure 2a). The mean particle diameter of nano-C_{60} produced by the THF method (65 mg/l) was 168.7 ± 18.1 nm ($R = 0.997$) (Figure 2b). The

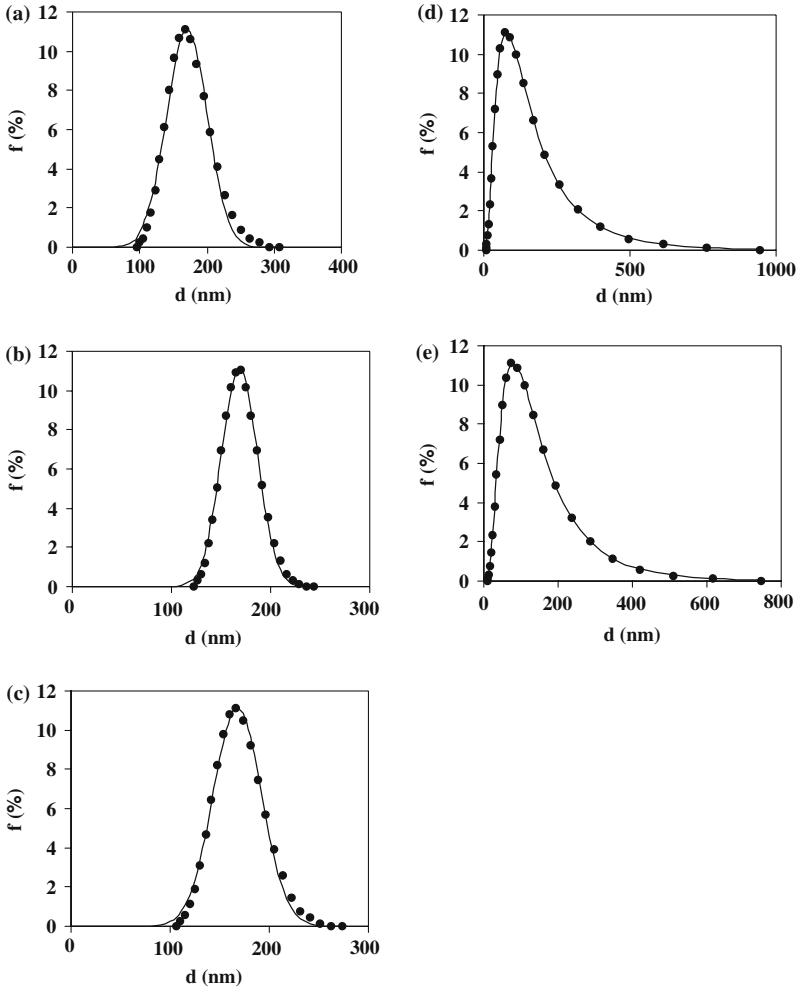

Figure 2. Particle size distribution of nano-C_{60}. *d* (nm) is the diameter of nano-C_{60}particles; *f* (%) is the fraction of scattered light intensity. ●, experimental data from photon correlation spectroscopy; lines, model fitting curves from Sigma-Plot. (a) nano-C_{60} prepared by sonication method (48 mg/l); (b) nano-C_{60} prepared by THF method (65 mg/l); (c) nano-C_{60} (65 mg/l) after adsorption, filtration and resuspension; (d) nano-C_{60} prepared by THF method (12.5 mg/l); (e) nano-C_{60} (12.5 mg/l), after adsorption, filtration and resuspension.

particle size distribution of nano-C_{60} particles produced by the THF method at 12.5 mg/l was fitted with a Log-normal distribution function. The mean natural logarithm particle diameter was 4.34 ± 0.8, or d_{mean} = 76.6 nm, with R = 1.000 (Figure 2d). The difference in particle sizes of the two THF preparations appears to be related to a slight difference in mixing, water addition, and the extent of rotary evaporation (Fortner et al., 2005). However, all of these nano-C_{60} samples appeared to be stable, non-aggregating, non-settling aqueous suspensions. After adsorption, filtration and resuspension, the mean of particle size distribution for the sample with 65 mg/l of nano-C_{60} was 167.9 ± 24.4 nm (Figure 2c), i.e., negligible change. The particle size distribution of nano-C_{60} particles (12.5 mg/l) after adsorption, filtration and resuspension was fitted with a Log-normal distribution function, with the mean natural logarithm particle diameter of 4.38 ± 0.7, or d_{mean} = 79.6 nm (R = 1.000, Figure 2e).

Adsorption of naphthalene to C_{60} with different aggregation forms

In the authors' previous paper, adsorption of naphthalene to 'C_{60} large aggregates' (20–50 μm) and 'C_{60} small aggregates' (1–3 μm) was studied (Cheng et al., 2004); data are shown in Figure 3 for the purpose of comparison. A linear isotherm in the form of $q = K_d C_w$ was observed for naphthalene adsorption to 'C_{60} large aggregates', where K_d (ml/g) denotes the solid–water distribution coefficient (Schwarzenbach et al., 2003), q (μg/g) is the mass of naphthalene per unit mass of C_{60} at equilibrium, and C_w (μg/ml) is the naphthalene concentration in the solution phase at equilibrium. A K_d value of $10^{2.39 \pm 0.02}$ ml/g was obtained from the linear isotherm. Naphthalene adsorption to 'C_{60} small aggregates' was fitted with a Freundlich isotherm $q = 10^{4.28 \pm 0.04}\ C_w^{0.45 \pm 0.05}$ (Figure 3). The adsorption of naphthalene to nano-C_{60} (sample numbers 1.1 to 1.7) can be fitted with a linear isotherm with $K_d = 10^{3.70 \pm 0.01}$ ml/g. The K_d value observed from Ballesteros et al. (Ballesteros et al., 2000) was one order of magnitude lower than that of 'C_{60} large aggregates', and three orders of magnitude lower than that of 'C_{60} small aggregates'.

It has been reported that black carbon particles can be quite porous and exhibit a high affinity for many organic contaminants, particularly for planar aromatic compounds such as PAHs (Goldberg, 1985; McGroddy et al., 1996; Gustafsson et al., 1997; Bucheli & Gustafsson, 2000). At C_w = 1 μg/ml, the K_d (ml/g) values for 'C_{60} large aggregates', 'C_{60} small aggregates', and nano-C_{60} are $10^{2.39 \pm 0.02}$, $10^{4.28 \pm 0.04}$, and $10^{3.70 \pm 0.01}$ ml/g, respectively. The corresponding K_d values for charcoals are similar and vary from $10^{2.44}$ to $10^{4.51}$ ml/g (Kleineidam et al., 2002; Zhu & Pignatello, 2005). Also, at the same conditions $K_d = 10^{3.03}$ ml/g is obtained for naphthalene partitioning to black carbon (Schwarzenbach et al., 2003). These results suggest that adsorption to nano-C_{60} is similar to that observed for some other forms of carbon.

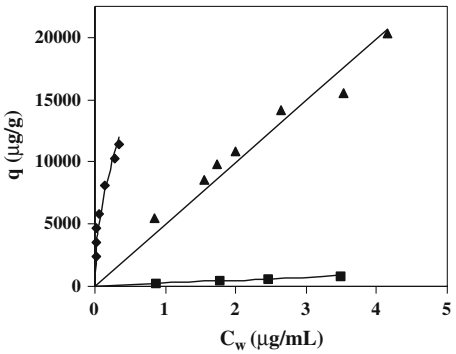

Figure 3. Naphthalene adsorption to 'C_{60} large aggregates', 'C_{60} small aggregates' and nano-C_{60} (sample numbers 1.1 to 1.7), ■, Naphthalene adsorption to 'C_{60} large aggregates'; ◆, Naphthalene adsorption to 'C_{60} small aggregates'; ▲, Naphthalene adsorption to nano-C_{60}.

Desorption of naphthalene from nano-C_{60} into water

Data of naphthalene adsorption to nano-C_{60} (sample numbers 1.1 to 1.7 and 3.1 and 3.2) and three steps of desorption for sample nos. 1.1, 1.3, 1.5, 3.1 and 3.2 are plotted in Figure 4. As is shown in Figure 4, within the time frame of these experiments, desorption of naphthalene from nano-C_{60} is highly hysteretic, i.e., desorption isotherm for each sample is not the reverse of the corresponding adsorption isotherm. For each sample, the solid–water distribution coefficient value ($K_d = q/C_w$) increased during the desorption process. The K_d values for the last desorption data points for the three samples are $10^{5.82}$, $10^{5.73}$ and $10^{5.74}$ ml/g, respectively, which are about two orders of

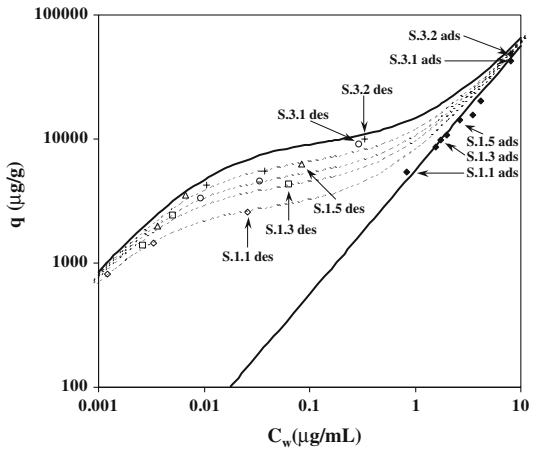

Figure 4. Adsorption and desorption of naphthalene with nano-C_{60}. ◆, adsorption of naphthalene to nano-C_{60} (sample numbers 1.1 to 1.7, 3.1 and 3.2);◇, □, Δ, ○ and +, desorption of naphthalene from nano-C_{60} (sample numbers 1.1, 1.3, 1.5, 3.1 and 3.2). Straight line, a linear isotherm in the form of $q(\mu g/g) = 10^{3.75}\ C_w$ (μg/ml); upper curve, model fitting curve assuming two-compartment desorption model (Eq. (1)). Dotted lines: two-compartment desorption model fitting curve with $f = 0.3$, 0.45, 0.55, and 0.7, respectively.

magnitude higher than the corresponding adsorption K_d values ($10^{3.75}$ ml/g). Cheng et al. (2004) also reported desorption hysteretis from 'C_{60} small aggregates' with desorption K_d values of $10^{5.95}$ and $10^{5.76}$ ml/g, similar to nano-C_{60}.

Artifacts, such as slow kinetics can easily be mistaken as sorption hysteresis. However, hysteresis has been reported in many studies of sorption to and from natural solids (Kan et al., 1994; Adamson & Gast, 1997; Kan et al., 1999; Lu & Pignatello, 2004). The kinetics of adsorption for naphthalene and dichlorobenzene should be orders of magnitude faster than for less soluble higher molecular weight PAHs and PCBs. We have observed that the adsorption of naphthalene to C_{60} thin films coated on glass walls was reversible, and desorption of naphthalene from 'C_{60} small aggregates' between 2 and 27 days showed no apparent change in solution phase naphthalene concentration, suggesting probable equilibrium (Cheng et al., 2004). Yet, the desorption of naphthalene from 'C_{60} small aggregates' (Cheng et al., 2004) and nano-C_{60} (Figure 4) apparently exhibit hysteresis. Nano-C_{60} is about 10–20 times smaller than 'C_{60} small aggregates'. The kinetics of adsorption reactions should be much faster in nano-C_{60} than in 'C_{60} small aggregates'. These data support the notion of a non-singular sorption isotherm for nano-C_{60}.

Desorption hysteresis of hydrophobic organic compounds has been observed in the adsorption and desorption studies with soils and sediments by numerous research groups (Di Toro & Horzempa, 1982; Karickhoff & Morris, 1985; Pignatello & Huang, 1991; Fu et al., 1994; Huang et al., 1998; Kan et al., 1998; Weber et al., 1998; Chen et al., 1999; Kan et al., 2000; Xia & Pignatello, 2001). Many mechanisms have been proposed to explain adsorption/desorption hysteresis in soils and sediments, including the 'entrapment' of the sorbed chemicals in the soil organic matter matrix following sorption (Carroll et al., 1994; Kan et al., 1998). Braida et al. (Braida et al., 2003) studied the sorption hysteresis of benzene in charcoal particles and concluded that the observed hysteresis is due to pore deformation by the solute and entrapment of some adsorbate as the polyaromatic scaffold collapses during desorption. Rathousky et al. observed hysteresis in the adsorption/desorption of cyclopentane vapor to C_{60} (Rathousky et al., 1993; Rathousky & Zukal, 2000). They explained the observed hysteresis by the penetration of cyclopentane molecules into the bulk of C_{60} crystals and possible entrapment of the adsorbate molecules. Interestingly, similar 'entrapment' was also found in the preparation of C_{60}, where toluene and some other aromatics were commonly used as extraction solvents. Traces of toluene or other solvents were often found entrapped, or intercalated, in the C_{60} lattice after removal of bulk toluene (Taylor, 1999).

Numerous theories and models have been used to express the general notion that with soil organic contaminants sorption and desorption are often different processes. Kan et al. proposed a two-compartment desorption model (Kan et al., 1998; Chen et al., 2002). The basic concept of this model is that both sorption and desorption are biphasic, consisting of two compartments, each with unique equilibrium and kinetic characteristics. In most cases, adsorption and desorption of organic contaminants at high initial concentrations (up to aqueous solubility) may be associated with the first compartment, while at low concentration ranges most of adsorption and desorption may be associated with the second compartment. According to

Table 1. DED model parameters for naphthalene (naph) and 1,2-dichlorobenzene (1,2-DCB) adsorption (ads) and desorption (des) with nano-C_{60}

Sorbate	ads/des	Sigma-Plot Derived Parameters			$R^{2\,a}$
		log K_d^{1st} (ml/g)	log K_d^{2nd} (ml/g)	log q_{max}^{2nd} (μg/g)	
naph	ads[b]	3.75 ± 0.01[c]			0.972
	des		5.90 ± 0.04	3.91 ± 0.01	0.996
1,2-DCB	ads	3.48 ± 0.01			0.994
	des		5.68 ± 0.08	3.98 ± 0.03	0.977

[a] Correlation coefficients.
[b] Adsorption data were used to determine K_d^{1st} from the first term of Eq. (1) using Sigma-Plot. Desorption data and K_d^{1st} determined from adsorption were used to determine K_d^{2nd} and q_{max}^{2nd} values with by fitting the data to Eq. (1) using Sigma-Plot.
[c] The number after ± is one standard deviation for each parameter.

the two-compartment desorption model, adsorption/desorption isotherm can be described by the following equation:

$$q = K_d^{1st} C_w + \frac{K_d^{2nd} f q_{max}^{2nd} C_w}{f q_{max}^{2nd} + K_d^{2nd} C_w} \quad (1)$$

where K_d^{1st} and K_d^{2nd} are solid–water distribution coefficients for the first and the second compartment; and q_{max}^{2nd} (μg/g) is defined as a maximum sorption capacity for the second compartment. The factor f ($0 \le f \le 1$) denotes the fraction of the second compartment that is filled at the time of exposure. At higher aqueous naphthalene concentrations, q is related to aqueous concentration C_w by a simple linear isotherm; and at lower aqueous naphthalene concentrations, q is related to aqueous concentration C_w by a Langmuir-type isotherm. In Figure 4, naphthalene adsorption and desorption data with nano-C_{60} were fitted with this two-compartment model. Adsorption data were fitted with a linear isotherm: q (μg/g) = $10^{3.75}$ C_w (μg/ml), the straight line in Figure 4. The upper curve is a curve fitted with Eq. (1), with K_d^{1st} from adsorption isotherm and $f = 1$. Data fitting was accomplished by Sigma-Plot; logarithmic values of fitted parameters, K_d^{1st} (ml/g), K_d^{2nd} (ml/g), and q_{max}^{2nd} (μg-naphthalene/g-C_{60}), are listed in Table 1. The dotted lines in Figure 4 are the fitted curves considering that the maximum sorption capacity in the second compartment is only partially saturated (f = 0.3, 0.45, 0.55, and 0.7, respectively). When C_w is close to one-half of the sorbate solubility, f can be assumed to be equal to one.

For soils and sediments, K_{oc}^{2nd} is the organic carbon normalized solid–water distribution coefficient for the second compartment. Note that: $K_d^{2nd} = K_{oc}^{2nd} \cdot OC$, where OC is the organic carbon content of the soil or sediment. For the C_{60} particles OC = 1.0 and therefore $K_d^{2nd} = K_{oc}^{2nd}$. It was reported by Kan et al. (1998) and Chen et al. (2002) that for many sediments/adsorbate combinations K_{oc}^{2nd} has been found to be a single constant, $K_{oc}^{2nd} = 10^{5.92 \pm 0.16}$ (ml/g). The K_d^{2nd} value obtained from model fitting of all experimental data of naphthalene adsorption and desorption with nano-C_{60} in Figure 4 was: $K_d^{2nd} = 10^{5.90 \pm 0.04}$ ml/g, almost identical to the value K_{oc}^{2nd} for soils. This consistency might suggest a common mechanism.

Adsorption of 1,2-DCB to nano-C_{60} and desorption into water

Adsorption and desorption of 1,2-dichlorobenzene (1,2-DCB) with nano-C_{60} were conducted similarly to the ones with naphthalene. Dichlorobenzene adsorption and desorption data for sample numbers 2.1 to 2.3 are plotted in Figure 5. Adsorption data were fitted with a linear isotherm, q (μg/g) = $10^{3.48 \pm 0.01}$ C_w (μg/ml). Data for three steps of desorption for each sample are plotted in the figure as well. Data were fitted with Eq. (1) and the upper curve in Figure 5 is the isotherm predicted with two-compartment desorption model. Parameters were obtained from Sigma-Plot and are listed in Table 1. The dotted lines in Figure 5 are model predictions (Eq. (1)) at f = 0.2, 0.55, and 0.7, respectively. It can be seen from Table 1 that the values of K_d^{1st}(ml/g), K_d^{2nd}(ml/g), and q_{max}^{2nd} for 1, 2-DCB adsorption and desorption with nano-C_{60} are similar to the corresponding values for that of

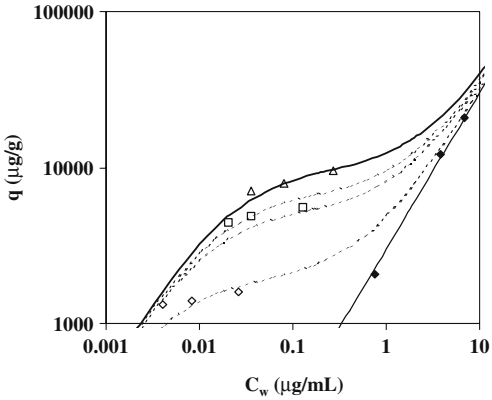

Figure 5. Adsorption and desorption of 1,2-DCB with nano-C_{60}. ◆, adsorption of 1,2-DCB to nano-C_{60} (sample numbers 2.1 to 2.3); ◇, □, Δ, desorption of 1,2-DCB from nano-C_{60} (sample numbers 2.1 to 2.3). Straight line, a linear isotherm in the form of q (μg/g) = $10^{3.48}$ C_w (μg/ml); upper curve, model fitting curve assuming two-compartment desorption model (Eq. (1)). Dotted lines: two-compartment desorption model fitting curve with f = 0.2, 0.55, and 0.7, respectively.

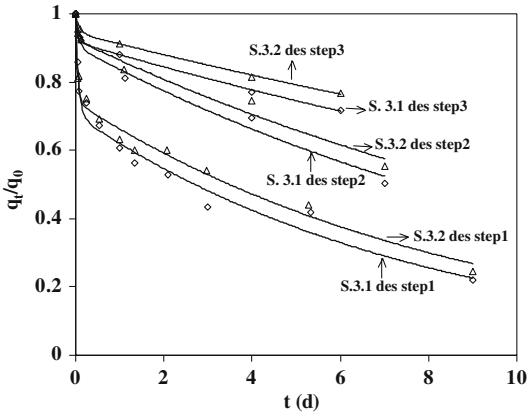

Figure 6. Plot of q_t/q_0 vs. t (days) for naphthalene desorption from nano-C_{60} (sample numbers 3.1 and 3.2). ◇, sample number 3.1; Δ, sample number 3.2. Solid lines were obtained from Sigma-Plot using the two-compartment first-order kinetics model (Eq. (2)).

naphthalene, as would be expected from the similar K_{ow} values between 1,2-DCB and naphthalene.

Desorption kinetics of naphthalene desorption from nano-C_{60}

The recorded concentrations of naphthalene desorption from nano-C_{60} with time were fitted with the empirical two-compartment first-order kinetics model (Cornelissen et al., 1997):

$$q_t/q_0 = F_1 e^{-k_1 t} + F_2 e^{-k_2 t} \quad (2)$$

in which q_t and q_0 (μg/g) are the C_{60}-adsorbed naphthalene concentrations at time t (day) and at the start of the experiment, respectively; F_1 and F_2 are the fractions of naphthalene present in the two kinetically different desorbing compartments; k_1 and k_2 (day^{-1}) are the first-order rate constants for the two desorption compartments.

In Figure 6 q_t/q_0 vs. time (t, days) for desorption of naphthalene from nano-C_{60} (sample numbers 3.1 and 3.2) are plotted (adsorption data for sample numbers 3.1 and 3.2 are included in Figure 4). The solid lines were obtained by curve fitting with Sigma-Plot to the two compartment first-order kinetic model (Eq. (2)). The parameters obtained by Sigma-Plot curve fitting are listed in Table 2.

It is shown that desorption data are fitted well with the two-compartment kinetics model. The standard deviation of k_1 values is large at the second and third desorption steps, since the majority of the adsorbed naphthalene is in the slow desorption domain. Three-step desorption experiments were conducted to both samples and with each step, desorption data were fitted with Eq. (2), which assumes a rapidly desorbed compartment and a slowly desorbed compartment. In the first desorption step for both samples, the fraction of naphthalene in the first compartment is relatively high (F_1 = 29.63 and 25.81%). In the second and third desorption steps, over 90% of the desorption occurred from the second compartment ($F_2 \geq 90\%$). This indicates that at desorption step 1, a larger fraction of the sorbate mass desorb from the rapid compartment, while at desorption step 2 and 3, sorbate mass desorb primarily from the slow desorption compartment. The rate constants for desorption from the first compartment (k_1) are relatively high, from 11.80 to 27.40 day^{-1}, while rate constants for desorption from the second compartment (k_2) range from 0.04 to 0.13 day^{-1}, more than two orders of magnitude lower than the corresponding k_1 value for each desorption step. It can been seen from Figure 6 that for each desorption step, the slopes of the

Table 2. Parameters of fitting the desorption kinetics data of naphthalene from nano-C_{60} to Eq. (2) using Sigma-Plot

	Sigma-Plot derived parameters				
	F_1	k_1 (d^{-1})	F_2	k_2 (d^{-1})	R^2
Sample No. 3.1					
Des step 1	0.296 ± 0.023	14.348 ± 4.020	0.704	0.126 ± 0.014	0.98
Des step 2	0.095 ± 0.031	14.172 ± 12.086	0.905	0.078 ± 0.009	0.989
Des step 3	0.083 ± 0.005	15.532 ± 3.529	0.917	0.043 ± 0.001	0.999
Sample No. 3.2					
Des step 1	0.258 ± 0.019	21.067 ± 6.151	0.742	0.113 ± 0.010	0.982
Des step 2	0.076 ± 0.027	27.396 ± 36.057	0.924	0.068 ± 0.008	0.981
Des step 3	0.056 ± 0.004	11.804 ± 2.970	0.944	0.035 ± 0.001	0.999

q_t/q_0 vs. t curves decrease gradually with time, indicating greater and greater resistance to desorption.

The last datum point for each desorption step of sample numbers 3.1 and 3.2 are also plotted in Figure 4 and are consistent with the two-compartment desorption model (Eq. (1)). Results of naphthalene desorption kinetics experiments with nano-C_{60} are consistent with the desorption results of 'C_{60} small aggregates' reported previously (Cheng et al., 2004).

Conclusions

The study of adsorption and desorption of naphthalene and 1,2-dichlorobenzene with C_{60} is reported in this paper. The virtually water-insoluble C_{60} can be dispersed in water and form water-stable nanoscale aggregates (nano-C_{60}), with negative surface charges. The different sizes of C_{60} aggregates, formed under different conditions, could affect the adsorption of naphthalene by orders of magnitude. Desorption of both naphthalene and 1,2-dichlorobenzene from nano-C_{60} exhibits hysteresis, and along with adsorption data, was described by a two-compartment desorption model. Kinetics data of naphthalene desorption from nano-C_{60} also indicated that desorption of naphthalene from C_{60} aggregates is composed of two compartments: a labile desorption compartment, where naphthalene can be readily desorbed; and a resistant desorption compartment, where naphthalene may be entrapped in C_{60} aggregates and desorption is hindered.

Acknowledgements

The financial supports of the National Science Foundation through the Center for Biological and Environmental Nanotechnology [EEC-0118007], U.S. EPA ORD/NCER/STAR nanotechnology program, U.S. EPA Hazardous Substance Research Center/South & Southwest Region, and Rice University Brine Chemistry Consortium of companies: Aramco, Baker-Petrolite, Champion Technologies, Inc., ChevronTexaco, Inc., ConocoPhillips, Inc., Marathon Oil, Nalco, Occidental Oil and Gas, are greatly appreciated.

References

Accardi-Dey A. & P.M. Gschwend, 2002. Assessing the combined roles of natural organic matter and black carbon as sorbents in sediments. Environ. Sci. Technol. 36(1), 21–29.

Adamson A.W. & A.P. Gast, 1997. Physical Chemistry of Surfaces. New York, NY, USA: John Wiley & Sons Inc.

Alargova R.G., S. Deguchi & K. Tsujii, 2001. Stable colloidal dispersions of fullerenes in polar organic solvents. J. Am. Chem. Soc. 123, 10460–10467.

Allen-King R.M., P. Grathwohl & W.P. Ball, 2002. New modeling paradigms for the sorption of hydrophobic organic chemicals to heterogeneous carbonaceous matter in soils, sediments, and rocks. Adv.Water Resour. 25, 985–1016.

Andersson T., K. Nilsson, M. Sundahl, G. Westman & O. Wennerstrom, 1992. C_{60} embedded in γ cyclodextrin: A water-soluble fullerene. J. Chem. Soc., Chem. Commun. 8, 604–607.

Andrievsky G.V., V.K. Klochkov, A.B. Bordyuh & G.I. Dovbeshko, 2002. Comparative anylysis of two aqueous-colloidal solutions of C_{60} fullerene with help of FTIR reflectance and UV–Vis spectroscopy. Chem. Phys. Lett. 364, 8–17.

Andrievsky G.V., V.K. Klochkov, E.L. Karyakina & N.O. Mchedlov-Petrossyan, 1999. Studies of aqueous colloidal solutions of fullerene by electron microscopy. Chem. Phys. Lett. 300, 392–396.

Andrievsky, G.V., M.V. Kosevich, O.M. Vovk, V. S. Shelkovsky & L.A. Vashchenko, 1995. On the production of an aqueous colloidal solution of fullerenes. J. Chem. Soc., Chem. Commun. 1281–1282.

Ballesteros E., M. Gallego & M. Valcarcel, 2000. Analytical potential of fullerene as adsorbent for organic and organometallic compounds from aqueous solutions. J. Chromatogr. A 869, 101–110.

Beeby, A., J. Eastoe & R.K. Heenan, 1994. Solubilisation of C_{60} in aqueous micellar solution. J. Chem. Soc., Chem. Commun. 173–175.

Bensasson R.V., E. Bienvenue, M. Dellinger, S. Leach & P. Seta, 1994. C_{60} in model biological systems. A Visible-UV absorption study of solvent-dependent parameters and solute aggregation. J. Phys. Chem. 98, 3492–3500.

Borm P.J.A., 2002. Particle toxicology: From coal mining to nanotechnology. Inhalation Toxicol. 14, 311–324.

Braida W.J., J.J. Pignatello, Y. Lu, P.I. Ravikovitch, A.V. Neimark & B. Xing, 2003. Sorption Hysteresis of Benzene in Charcoal Particles. Environ. Sci. Technol. 37(2), 409–417.

Brettreich M. & A. Hirsch, 1998. A highly water-soluble dendro[60]fullerene. Tetrahedron Lett. 39(18), 2731–2734.

Bucheli T.D. & O. Gustafsson, 2000. Quantification of the soot-water distribution coefficient of PAHs provides mechanistic basis for enhanced sorption observations. Environ. Sci. Technol. 34, 5144–5151.

Carroll K.M., M.R. Harkness, A.A. Bracco & R.R. Balcarcel, 1994. Application of a permeant/polymer diffusional model to the desorption of polychlorinated biphenyls from Hudson River sediments. Environ. Sci. Technol. 28(2), 253–258.

Chen W., A.T. Kan, G. Fu, L.C. Vignona & M.B. Tomson, 1999. Adsorption-desorption behaviors of hydrophobic organic compounds in sediments of Lake Charles, Louisiana, USA. Environ. Toxicol. Chem. 18(8), 1610–1616.

Chen W., A.T. Kan, C.J. Newell, E. Moore & M.B. Tomson, 2002. More realistic soil cleanup standards with dual-equilibrium desorption. Ground Water 40(2), 153–164.

Cheng X., A.T. Kan & M.B. Tomson, 2004. Naphthalene adsorption and desorption from aqueous C_60 fullerene. J. Chem. Eng. Data 49, 675–683.

Chiou C.T. & D.E. Kile, 1998. Deviation from sorption linearity on soils of polar and nonpolar organic compounds at low relative concentrations. Environ. Sci. Technol. 32(3), 338–343.

Chiou C.T., L.J. Peters & V.H. Freed, 1979. A physical concept of soil–water equilibria for nonionic organic compounds. Science 206, 831–832.

Chun Y., G. Sheng, C.T. Chiou & B. Xing, 2004. Composition and sorptive properties of crop residue-derived chars. Environ. Sci. Technol. 38, 4649–4655.

Colvin V.L., 2003. The potential environmental impact of engineered nanomaterials. Nat. Biotechnol. 21(10), 1166–1170.

Cornelissen G. & O. Gustafsson, 2005. Importance of unburned coal carbon, black carbon, and amorphous organic carbon to phenanthrene sorption in sediments. Environ. Sci. Technol. 39, 764–769.

Cornelissen G., P.C.M. Van Noort, J.R. Parsons & H.A.J. Govers, 1997. Temperature dependence of slow adsorption and desorption kinetics of organic comounds in sediments. Environ. Sci. Technol. 31(2), 454–460.

Dagani R., 2003. Nanomaterials: Safe or unsafe? Chem. Eng. News 81, 30.

Deguchi S., R.G. Alargova & K. Tsujii, 2001. Stable Dispersions of Fullerenes, C_{60} and C_{70}, in water. Preparation and characterization. Langmuir 17(19), 6013–6017.

Di Toro D.M. & L.M. Horzempa, 1982. Reversible and resistant components of PCB adsorption-desorption: Isotherms. Environ. Sci. Technol. 16(9), 594–602.

Fortner J.D., J.C. Falkner, E.M. Hotze, D.Y. Lyon, C.M. Sayes, K.D. Ausman, V.L. Colvin & J.B. Hughes,. 2005. C_{60} Aggregates in Water: Formation Dynamics and Further Characterization. San Diego, CA, United States: 229th ACS National Meeting.

Fu G., A.T. Kan & M.B. Tomson, 1994. Adsorption and desorption hysteresis of PAHs in surface sediment. Environ. Toxicol. Chem. 13(10), 1559–1567.

Ghosh U., J.T. Zimmerman & R.G. Luthy, 2003. PCB and PAH speciation among particle types in contaminated harbor sediments and effects on PAH bioavailability. Environ. Sci. Technol. 37, 2209–2217.

Goldberg E.D., 1985. Black Carbon in the Environment. New York, USA: John Wiley & Sons, Inc.

Gustafsson O., F. Haghseta, C. Chan, J. Macfarlane & P.M. Gschwend, 1997. Quantification of the Dilute Sedimentary Soot Phase: Implications for PAH Speciation and Bioavailability. Environ. Sci. Technol. 31, 203–209.

Heymann D., S.M. Bachilo, R.B. Weisman, F. Cataldo, R.H. Fokkens, N.M.M. Nibbering, R.D. Vis & L.P.F. Chibante, 2000. $C_{60}O_3$, a fullerene ozonide: Synthesis and dissociation to $C_{60}O$ and O_2. J. Am. Chem. Soc. 122, 11473–11479.

Huang W. & W.J.J. Weber, 1997. A distributed reactivity model for sorption by soils and sediments: 10. Relationships between desorption, hysteresis, and the chemical characteristics of organic domains. Environ. Sci. Technol. 31(9), 2562–2569.

Huang W., H. Yu & W.J.J. Weber, 1998. Hysteresis in the sorption and desorption of hydrophobic organic contaminants by soils and sediments. 1. A comparative anylysis of experimental protocols. J. Contam. Hydrol. 31, 129–148.

James G., D.A. Sabatini, C.T. Chiou, D. Rutherford, A.C. Scott & H.K. Karapanagioti, 2005. Evaluating phenanthrene sorption on various wood chars. Water Resour. 39, 549–558.

Jenekhe S.A. & X.L. Chen, 1998. Self-assembled aggregates of rod-coil block copolymers and their solubilization and encapsulation of fullerenes. Science 279(5358), 1903–1907.

Kan A.T., W. Chen & M.B. Tomson, 1999. Desorptino kinetics of neutral hydrophobic organic compounds from field-coontaminated sediment. Environ. Pollut. 108, 81–89.

Kan A.T., W. Chen & M.B. Tomson, 2000. Desorption kinetics of neutral hydrophobic organic compounds from field-contaminated sediment. Environ. Pollut. 108, 81–89.

Kan A.T., G. Fu, M. Hunter, W. Chen, C.H. Ward & M.B. Tomson, 1998. Irreversible adsorption of neutral organic hydrocarbons-experimental observations and model predictions. Environ. Sci. Technol. 32, 892–902.

Kan A.T., G. Fu & M.B. Tomson, 1994. Adsorption/desorption hysteresis in organic pollutant and soil/sediment interaction. Environ. Sci. Technol. 28, 859–867.

Karickhoff S.W., D.S. Brown & T.A. Scott, 1979. Sorption of hydrophobic pollutants on natural sediments. Water Resour. 13, 241–248.

Karickhoff S.W. & K.R. Morris, 1985. Sorption dynamics of hydrophobic pollutants in sediment suspensions. Environ. Toxicol. Chem. 4(4), 469–479.

Kleineidam S., C. Schuth & P. Grathwohl, 2002. Solubility-normalized combined adsorption-partitioning sorption isotherms for organic pollutants. Environ. Sci. Technol. 36, 4689–4697.

Kratschmer W., K. Fostiropoulos & D.R. Huffman, 1990. The infrared and ultraviolet absorption spectra of laboratory-produced carbon dust: Evidence for the presence of the C_{60} molecule. Chem. Phys. Lett. 170, 167–170.

Lai D.T., M.A. Neumann, M. Matsumoto & J. Sunamoto, 2000. Complexation of C_{60} Fullerene with Cholesteryl Group-Bearing Pullulan in Aqueous Medium. Chem. Lett. 1, 64–65.

Lecoanet H.F. & M.R. Wiesner, 2004. Velocity effects on fullerene and oxide nanoparticle deposition in porous media. Environ. Sci. Technol. 38, 4377–4382.

Lu Y. & J.J. Pignatello, 2004. History-dependent sorption in humic acids and a lignite in the context of a polymer model for natural organic matter. Environ. Sci. Technol. 38, 5853–5862.

McGroddy S.E. & J.W. Farrington, 1995. Sediment porewater partitioning of polycyclic aromatic hydrocarbons in three cores from Boston Harbor, Massachusetts. Environ. Sci. Technol. 29(6), 1542–1550.

McGroddy S.E., J.W. Farrington & P.M. Gschwend, 1996. Comparison of the in situ and desorption of sediment–water partitioning of polycyclic aromatic hydrocarbons and polychlorinated biphenyls. Environ. Sci. Technol. 30(1), 172–177.

Mchedlov-Petrossyan N.O., V.K. Klochkov & G.V. Andrievsky, 1997. Colloidal dispersions of fullerene C_{60} in water: Some properties and regularities of coagulation by electrolytes. J. Chem. Soc., Faraday Trans. 93(24), 4343–4346.

Mchedlov-Petrossyan N.O., V.K. Klochkov, G.V. Andrievsky & A.A. Ishchenko, 2001. Interaction between colloidal particles of C_{60} hydrosol and cationic dyes. Chem. Phys. Lett. 341, 237–244.

Nguyen T.H., I. Sabbah & W.P. Ball, 2004. Sorption nonlinearity for organic contaminants with diesel soot: Method develpment and isotherm interpretation. Environ. Sci. Technol. 38(13), 3595–3603.

Pignatello J.J., 1989. Slowly reversible sorption of aliphatic halocarbons in soils. I. Formation of residual fractions. Environ. Toxicol. Chem. 9, 1107–1115.

Pignatello J.J. & L.Q. Huang, 1991. Sorptive reversibility of atrazine and metolachlor residues in field soil samples. J. Environ. Qual. 20(1), 222–228.

Pignatello J.J. & B. Xing, 1996. Mechanisms of slow sorption of organic chemicals to natural particles. Environ. Sci. Technol. 30(1), 1–11.

Rathousky J., J. Starek, A. Zukal & W. Kratschmer, 1993. Uptake of cyclopentane vapours in a fullerite powder. Fullerene Sci. Technol. 1(4), 575–582.

Rathousky J. & A. Zukal, 2000. Adsorption of krypton and cyclopentane on C60: An experimental study. Fullerene Sci. Technol. 8(4&5), 337–350.

Ruoff R.S., D.S. Tse, R. Malhotra & D.C. Lorents, 1993. Solubility of fullerene (C60) in a variety of solvents. J. Phys. Chem. 97(13), 3379–3383.

Sano M., K. Oishi, T. Ishi-i & S. Shinkai, 2000. Vesicle formation and its fractal distribution by bola-amphiphilic [60]fullerene. Langmuir 16(8), 3773–3776.

Sayes C.M., J.D. Fortner, W. Guo, D. Lyon, A.M. Boyd, K.D. Ausman, Y.J. Tao, B. Sitharaman, L.J. Wilson, J.B. Hughes, J.L. West & V.L. Colvin, 2004. The differential cytotoxicity of water-soluble fullerenes. Nano Lett. 4(10), 1881–1887.

Schwarzenbach R.P., P.M. Gschwend & D.M. Imboden, 2003. Environmental Organic Chemistry. Hoboken, New Jersey: John Wiley & Sons, Inc.

Scrivens W.A., J.M. Tour, K.E. Creek & L. Pirisi, 1994. Synthesis of ^{14}C-labeled C_{60}, its suspension in water, and its uptake by human keratinocytes. J. Am. Chem. Soc. 116, 4517–4518.

Setton R., P. Bernier & S. Lefrant, 2002. Carbon Molecules and Materials. New York: Taylor and Francis.

Steinberg S.M., J.J. Pignatello & B.L. Sawhney, 1987. Persistence of 1,2-dibromoethane in soils: Entrapment in intraparticle micropores. Environ. Sci. Technol. 21(12), 1201–1208.

Taylor R., 1999. Lecture Notes on Fullerene Chemistry, A Handbook for Chemists. UK: Imperial College Press London.

Weber W.J.J., W. Huang & H. Yu, 1998. Hysteresis in the sorption and desorption of hydrophobic organic contaminants by soils and sediments. 2. Effects of soil organic matter heterogeneity. J. Contam. Hydrol. 31, 149–165.

Wei X., M. Wu, L. Qi & Z. Xu, 1997. Selective solution-phase generation and oxidation reaction of C_{60}^{n-} (n = 1,2)and formation of an aqueous colloical solution of C_{60}. J. Chem. Soc., Perkin Trans. 2, 1389–1393.

Weisman R.B., D. Heymann & S.M. Bachilo, 2001. Synthesis and characterization of the "missing" oxide of C_{60}: [5,6]-open $C_{60}O$. J. Am. Chem. Soc. 123, 9720–9721.

Xia G. & J.J. Pignatello, 2001. Detailed sorption isotherms of polar and apolar compounds in a high-organic soil. Environ. Sci. Technol. 35, 84–94.

Zhu D., S. Hyun, J.J. Pignatello & L.S. Lee, 2004. Evidence for π–π electron donor–acceptor interactions between π-donor aramatic compounds and π-acceptor sites in soil organic matter through pH effects on sorption. Environ. Sci. Technol. 38, 4361–4368.

Zhu D. & J.J. Pignatello, 2005. Characterization of aromatic compound sorptive interactions with black carbon (charcoal) assisted by graphite as a model. Environ. Sci. Technol. 39(7), 2033–2041.